Catal Lett (2012) 142:830–837
DOI 10.1007/s10562-012-0831-3

Metal Support Interactions in Co_3O_4/Al_2O_3 Catalysts Prepared from w/o Microemulsions

N. Fischer · M. Minnermann · M. Baeumer · E. van Steen · M. Claeys

Received: 23 March 2012 / Accepted: 16 April 2012 / Published online: 8 May 2012

Abstract To obtain nano-sized metal and metal salt crystallites with a narrow size distribution synthesis methods utilizing water in oil (w/o) microemulsions, i.e. reverse micelles, have been widely applied and reported in literature. In this study we show the effect of support addition at different stages of the reverse micelle based preparation of cobalt oxide on alumina model catalysts. All catalysts were characterized with X-ray powder diffraction and Raman spectroscopy indicating the presence of Co_3O_4 on the Al_2O_3 support. Studies of the reduction behaviour and X-ray photoelectron spectroscopy however revealed the presence of difficult to reduce cobalt aluminate species in the samples where the support was added during or shortly after the precipitation step in the synthesis process. It can therefore be assumed that if the alumina support is added to the reverse micelle solution unprecipitated Co^{2+} ions and partially dissolved Al^{3+} combine and form cobalt aluminates. In the preparations where the solid cobalt precipitates are recovered from the microemulsion and then supported on the carrier, no metal-aluminate formation could be observed. This study therefore gives important information how metal-support interaction can be affected during catalyst preparation using reverse micelles.

N. Fischer · E. van Steen · M. Claeys (✉)
Centre for Catalysis Research and c*change (DST-NRF Centre of Excellence in Catalysis), Department of Chemical Engineering, University of Cape Town, Cape Town 7701, South Africa
e-mail: michael.claeys@uct.ac.za

M. Minnermann · M. Baeumer
Institute of Applied and Physical Chemistry, University of Bremen, Leobener Str. NW2, 28359 Bremen, Germany

Keywords Cobalt aluminates · Reverse micelle · Raman spectroscopy · XRD · XPS

1 Introduction

Microemulsions are thermodynamically stable mixtures of an aqueous, an oil and a surfactant phase [1–5]. In the oil rich area of the ternary phase diagram of this mixture, small water droplets, stabilized by a surfactant layer, form in the oil continuum referred to as reverse micelles. Although these confined water droplets have been shown to undergo exchange of matter through fusion and separation [6, 7] the reverse micelles have been successfully used as nano-reactors/templates for the formation of precipitates, as the size, geometry and nature of the precipitate is dependent on the size and nature of the reverse micelle [8–14]. While long known for its suitability to produce nano-sized metal/metal salt crystallites, the use of reverse micelles for the preparation of heterogeneous model catalysts has first been postulated only in the early 1970s [15] and it has since then been used by several researchers for a large number of microemulsion and metal precursor systems [3, 4].

In order to form the desired precipitate two main approaches are described in literature [3]:

- The preparation of two microemulsions that differ in the composition of the water core. One aqueous phase contains the metal precursor while the other contains a precipitation/reduction agent. After mixing the two reverse micelle systems, the micelles interact and form the desired precipitate within the confined geometry of the micelle.
- A single microemulsion is prepared with the dissolved metal precursor in the aqueous phase. The precipitation/

reduction agent is then added directly to this solution and leads to the precipitate.

For the synthesis of heterogeneous model catalysts the active phase is usually supported onto an inert carrier/support like SiO_2, Al_2O_3 or TiO_2. Although regarded as inert during the respective reaction conditions, supports have been described to influence the catalytic activity through the formation of crystalline phases in which atoms of the catalytically active material get incorporated in the crystal lattice of the support material [16]. In the Fischer–Tropsch synthesis for example cobalt on alumina is used as catalyst. With respect to the described interactions, the formation of cobalt aluminates can lead to a significant loss in catalytic activity.

In this study we compare support addition at different stages during the synthesis of a Co_3O_4/Al_2O_3 model catalyst via the reverse micelle method and the extent of interaction of Co^{2+} ions with the Al_2O_3 support resulting in the formation of the cobalt aluminates. These support addition effects on metal support interaction using reverse micelle derived have to our best knowledge not been studied in detail before.

2 Experimental

2.1 Chemicals

To prepare the supported cobalt nano crystallites the following chemicals were used: *n*-hexane and acetone supplied by KIMIX Ltd., Berol 050 (penta-ethyleneglycol-dodecylether PEGDE) supplied by Azko Nobel, cobalt nitrate ($Co(NO_3)_2{\cdot}6H_2O$) and 25 wt% ammonia solution from Sigma-Aldrich. The cobalt nitrate was dried in a desiccator over silica gel prior to its use as the cobalt precursor. The other chemicals were used as supplied. As the support material, commercially available alumina (Puralox, SCCa 5–150, Sasol Germany, $S_{BET} = 162\ m^2/g$, $V_{pore} = 0.47\ cm^3/g$, $đ_{pore} = 11.5$ nm, particle size = 150–200 μm) was used.

2.2 Preparation of Supported Cobalt Nano Crystallites

The microemulsion system chosen in this study is a mixture of an organic non-polar phase (*n*-hexane), an anionic surfactant (penta-ethylenglycol-dodecylether, PEGDE) and an aqueous phase. The so called reverse micelles form in the oil rich area of the ternary phase diagram. The stability region of the reverse micelles and its temperature dependency were determined previously [17].

The reverse micelles are formed at room temperature (25 °C) by mixing the oil and the surfactant in an appropriate glass vessel and stirring at room temperature for one hour. An aqueous cobalt nitrate solution then is added drop wise under stirring resulting in a clear pink solution. This solution is further stirred at 800 rpm on a magnetic stirring plate for 2 h before it is left to rest for 12 h. The compositions of the reverse micelle solutions used in this study are listed in Table 1.

Table 1 Composition of the microemulsions used to obtain CAT A–D samples

Catalyst	Hexane (g)	PEGDE (g)	Co-Sol.[a] (g)	Conc.[b] (mol/l)	ω (g/g)
CAT A	300	30.0	13.8	0.52	0.4
CAT B	400	40.0	17.0	0.20	0.4
CAT C	500	68.4	46.5	0.19	0.6
CAT D	500	68.4	29.2	0.15	0.4

[a] Cobalt solution

[b] Concentration of $Co(NO_3)_2{\cdot}6H_2O$ in the aqueous cobalt solution

2.2.1 Method A

The matching amount of dried alumina powder to obtain 5 wt% cobalt loading is added under stirring to the clear pink reverse micelle solution described earlier. Contrary to a previously described ruthenium system [18] no colour change, which would indicate the direct uptake of the cobalt onto the support, was observed. Ammonia solution is then added drop wise (NH_3:Co^{2+} ratio of 4:1) resulting in an instant colour change from pink to light green due to the formation of cobalt hydroxide species. The cobalt hydroxide does not settle in the preparation vessel as it is still entrapped in the geometry of the reverse micelle. The reverse micelles encapsulating the precipitated $Co(OH)_x$ are destabilised after 30 min of stirring via drop wise addition of acetone (volume of acetone to volume of microemulsion 1:1 upto 1:2). The resulting precipitate/Al_2O_3 mixture is washed thoroughly with acetone to remove residual surfactant. After decanting the acetone the solid is dried at 300 mbar and 60 °C in a rotary evaporator. The dry powder is calcined in a fluidized bed under air (approximately 50 ml_{Air}/min g (STP)) at 300 °C for 4 h.

2.2.2 Method B

The reverse micelle solution with the cobalt precursor is prepared as per method A. The NH_3 solution is added drop wise, i.e. before the support addition, and the mixture is left to react for 30 min under stirring. As previously described the colour of the solution changes instantly from pink to light green but remains clear, indicating the formation of cobalt hydroxides in the confinement of the reverse micelles. After the 30 min of reaction the alumina is added

followed by the drop wise addition of acetone to destabilize the reverse micelles. The resulting precipitate/Al_2O_3 mixture is then treated as described in method A.

2.2.3 Method C

The reverse micelle solution is prepared as described above and reacted with NH_3 solution. In contrast to method B the reverse micelles are destabilized via the addition of acetone without addition of alumina and the resulting $Co(OH)_x$ precipitate is washed extensively with acetone. The obtained precipitate is resuspended in acetone in an ultrasonic bath and alumina (matching amount to obtain 5 wt% Co loading) is added. The mixture is heated to 50 °C in an ultrasonic bath and dried under N_2 flow. The dry powder is calcined in a fluidized bed in air (approximately 50 ml_{Air}/min g (STP)) at 300 °C for 4 h.

2.2.4 Method D

The $Co(OH)_x$ precipitate is formed as described in method C and washed extensively. It is then dried at 130 °C in air for 12 h followed by a calcination at 200 °C in air for 5 h in an open Petri dish in an oven. The obtained Co_3O_4 particles are resuspended in water under ultrasonication. Al_3O_4 is added to the slurry and the mixture is dried at 200 mbar and 80 °C in a rotary evaporator.

2.3 Characterization Methods

The amount of cobalt loaded was determined using atomic absorption spectroscopy (AAS) (Varian SpectraAA 110). For this, 0.05 g of catalyst was digested in a mixture of HCl/HF, HNO_3 and $HClO_3$ and then diluted in water for analysis.

Raman spectroscopy was carried out in a Thermo Scientific Nicolet 5700 combined FT-IR/Raman instrument. To avoid sample heating of the dark coloured Co_3O_4/Al_2O_3 powder from the excitation laser, a small amount of sample was mixed with potassium bromide powder milled and pressed to a tablet prior to the scan.

X-ray powder diffraction (XRD) spectroscopy was carried out in a Bruker D8 Advance laboratory X-ray diffractometer equipped with a cobalt source ($\lambda_{K\alpha 1} = 0.178897$ nm) and a position sensitive detector (VÅNTEC-2000, Bruker AXS). To analyse the XRD spectra Rietveld refinement methods using TOPAS 4.2 (Bruker AXS) were applied. As the crystal structure of the alumina (predominantly consisting of γ-alumina) support is partially unknown an approach described by Scarlett and Madsen [19] for partially or not known crystal structures (PONKCS) was applied in order to obtain quantitative information from the XRD spectra.

The reduction behaviour of the oxidic model catalyst precursors was studied by means of temperature programmed reduction (TPR). TPR was carried out in a Micromeritics AutoChem 2950. An amount of 100 mg of sample was heated under a flow of 5 % H_2 in Ar (50 ml(NTP)/min) at a rate of 10 °C/min to 1,000 °C and kept at 1,000 °C for 2 h. The exhaust gas stream was analysed by a thermal conductivity detector (TCD) to monitor the H_2 consumption during the reduction.

The surface composition of the differently prepared catalysts was determined by X-ray photoelectron spectroscopy (XPS). For this purpose, the powder samples were introduced into an UHV analysis chamber (Omicron) using a transferable sample plate, on which the samples were fixed by means of a cabon sticky tape. The XPS analysis was carried out with a Leybold EA 10 plus analyser and a VG dual X-ray anode using Mg Kα radiation. Charging effects were corrected by referencing the BE scale to the C1s signal, which was set to 284.6 eV.

3 Results and Discussion

In all four preparation methods studied it was aimed to yield an alumina supported cobalt catalyst with a total cobalt loading of 5 wt%. Methods B–D indeed yield catalyst samples with the desired cobalt loading of approximately 5 wt% (see Table 2). The slightly lower loading of CAT A might be the result more intensive washing in this preparation procedure, causing the loss of cobalt hydroxide precipitate.

Raman spectroscopy allows the identification of the cobalt phases present in the studied samples by comparison of the scans with known samples or with data from literature [20–24]. The obtained spectra (see Fig. 1) compare well to the reference material Co_3O_4 (obtained via the calcination of precipitated cobalt hydroxide at 500 °C in air and identified with XRD) as well as to Co_3O_4 spectra reported in literature [21–23]. The spectra of CAT A and B display more intense peaks at wave lengths of approximately 200 cm^{-1} as well as wider peaks at a wavenumber of 700 cm^{-1}. Furthermore a shoulder is formed at a wavenumber of 500–510 cm^{-1}. These peak positions have previously been reported to correlate to the $CoAl_2O_4$ structure [20, 24]. No peaks for other cobalt phases such as

Table 2 Cobalt loading of studied samples obtained from AAS

Sample	Co wt% (AAS)
CAT A	4.0 ± 0.01
CAT B	5.1 ± 0.02
CAT C	4.7 ± 0.03
CAT D	5.0 ± 0.02

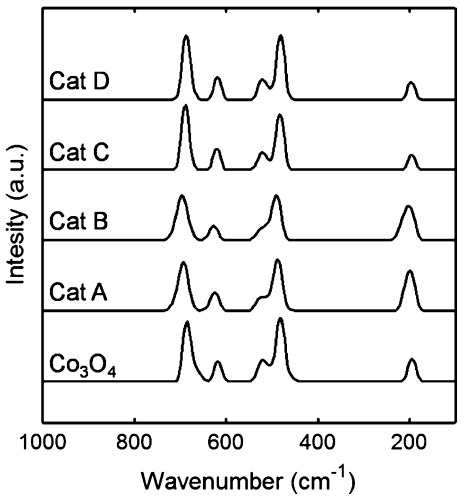

Fig. 1 Raman spectra of studied catalyst samples and spectrum of Co_3O_4 as reference material

$Co(OH)_2$ [23] or CoO [21] could be observed. It can therefore be concluded that the predominant cobalt phase on the surface of all catalyst samples after calcinations is the spinel Co_3O_4 oxide with possibly a small amount of $CoAl_2O_4$ present.

After the catalyst preparation the calcined samples were analysed using powder X-ray diffraction. From the diffraction patterns the different crystalline phases in a sample can be identified by comparison with known reference patterns (see Fig. 2). In addition to the amount of cobalt, the crystallite size does also influence the peak size and shape of the diffraction pattern of the metal oxide. Larger crystallites result in sharper and more intense peaks while smaller crystallites result in broad peaks with a low intensity. In all four preparation methods tested here it was aimed to yield cobalt oxide crystallites smaller than 15 nm. Due to the differences in the reverse micelle composition in the preparation process of the four studied samples (see Table 1) we do not expect the same crystallite sizes [17]. However, the crystallite size is at this stage only of secondary interest as the main focus lies on the nature of the cobalt phase and its behaviour during reduction/activation. A Rietveld refinement of the obtained experimental scans was conducted. This method entails the mathematical modeling of experimental diffraction patterns based on a convolution of known reference patterns/crystalline phases and instrument characteristics, and it allows determining quantitative identification of the phases composition and average sizes of the different crystallite phases. A further difficulty with the present cobalt oxide/alumina system is the partially unknown crystallite phase of the alumina support. Although mainly consisting of known and well studied γ-Al_2O_3, it is suspected that the present alumina also contains unknown amounts of the previously not studied δ phase of alumina. Traditional Rietveld refinement requires the input of all present crystalline phases including their respective space groups. This can not be done for the alumina used in this study. Scarlett and Madsen [19] developed a novel approach to apply Rietveld refinement methods to partially or not known crystal structures (PONKCS). Adapting this approach the cobalt oxide/alumina system can be fully analysed.

Figure 2 and Table 3 display the results obtained from XRD measurements and Rietveld refinement of the experimental spectra. Due to the low cobalt loadings, all scans are dominated by the diffraction pattern of the pure alumina support. From comparison of the experimental XRD traces with reported diffraction patterns, the only phase present besides the alumina support is Co_3O_4. The most prominent diffraction line of this phase is found at 43° 2θ (cobalt X-ray source with a wavelength of $\lambda = 0.178897$ nm). Rietveld refinement of the experimental data also confirms Co_3O_4 to be the only XRD visible phase present (i.e. crystalline and above critical crystallite size above $\sim$1–2 nm). The crystallite sizes shown in Table 3

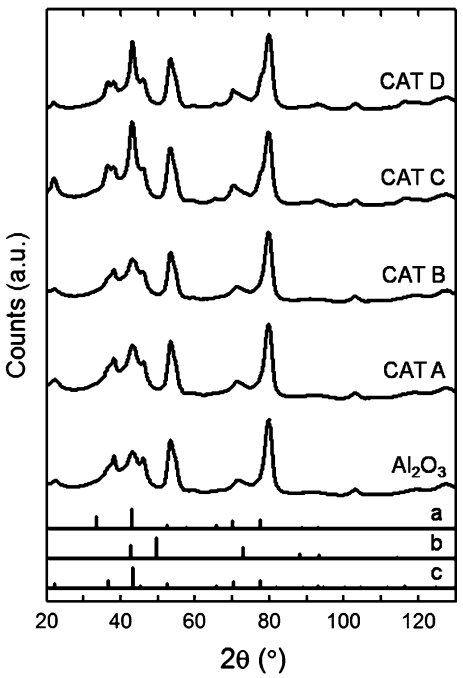

Fig. 2 XRD spectra of samples CAT A-D, pure Al_2O_3 and reference patterns of Co_3O_4 (*a*), CoO (*b*) and $CoAl_2O_4$ (*c*) ($\lambda = 0.178897$ nm)

Table 3 Average Co_3O_4 crystallite size obtained from Rietveld refinement using PONKCS approach

Sample	$d_{Co_3O_4}$ (nm)
CAT A	3.6
CAT B	3.4
CAT C	7.2
CAT D	9.9

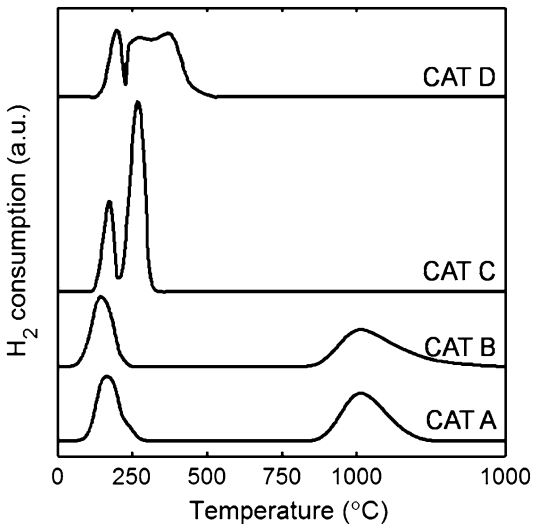

Fig. 3 TPR spectra of studied catalyst samples (CAT A–D)

reflect the differences in peak shape in the experimental patterns, with CAT D having the largest average Co_3O_4 crystallite size, 9.9 nm, and therefore resulting in the sharpest and most intense peak and CAT B having the smallest average Co_3O_4 crystallite size, 3.2 nm.

The TPR profiles of supported cobalt oxides have been studied extensively in literature [21, 24–31]. However, the peak identification is still discussed controversially. The TCD spectrum of the reduction of Co_3O_4 has been described by some as one peak [26, 28, 29, 31] while others consider two adjacent peaks [21, 24, 25, 27, 28, 30] indicating the two step reduction from Co_3O_4 to CoO followed by the reduction to metallic Co. Figure 3 shows the TPR profile of catalysts CAT A–D.

Catalyst samples CAT A and B show only one low temperature reduction peak around 200 °C with a small shoulder at temperatures of 250 °C. This peak can be assigned to the reduction of Co_3O_4, as identified by the XRD analysis, to Co^{2+}, which might undergo in comparison to Co^{3+} interactions with the support material, and further to metallic cobalt [26, 28, 29, 31]. A second peak at temperatures above 750 °C indicates the presence of strong interactions between Co^{x+} and the Al_2O_3 support [26, 28, 29, 31] as it is the case when cobalt is incorporated in the crystal lattice of alumina. Catalyst samples CAT C and D display two adjacent peaks between 200 and 500 °C which can be assigned to the two step reduction process of Co_3O_4. CAT C shows complete reduction at temperatures as low as 325 °C while CAT D is only fully reduced at 500 °C. This indicates a very low or no interaction of the alumina support with the cobalt phase in CAT C while some interaction seems to exist with sample CAT D. This difference in metal-support interaction can be explained by the differences in the preparation methods C and D. As Fig. 4

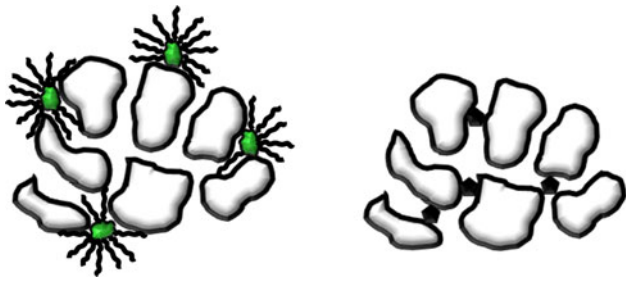

Fig. 4 Schematic representation of the combination of precipitate/Co_3O_4 crystallites and alumina support in preparation methods C and D. Residual surfactant hinders the cobalt hydroxide particles to enter the pore structure of the support (method C). Calcined Co_3O_4 crystallites can enter the pore structure and undergo stronger interactions with the support (method D)

depicts, in the case of method C the support is contacted with the precipitated cobalt phase prior to calcination. Despite extensive washing the precipitate is likely to still be covered with residual surfactant (PEGDE) from the reverse micelle solution at this stage. These surfactant/cobalt hydroxide particles may have larger diameters than the average pore diameter of the support of 11.5 nm [18, 22]. This results in the cobalt particles being deposited on the outer surface of the support structure and therefore they only have minimal contact with the alumina (see Fig. 5). In method D the precipitate of the reverse micelle solution is calcined and forms sub 10 nm Co_3O_4 crystallites. When these are contacted and dispersed onto the support they have the possibility to enter the pore structure of the alumina and therefore be in closer contact with the carrier material without forming, in bulk, new crystalline phases incorporating cobalt ions into the alumina lattice [16] in the form of cobalt aluminates. The formation of cobalt aluminates seem to have dominated in methods A and B where the support was added directly to the reverse micelle system (before or after precipitation). Here a very intimate contact of the cobalt precursor and the alumina existed and may have caused the observed effect.

The oxidation state of the cobalt oxide species was further studied with XPS (see Fig. 5). Additionally, pure Co_3O_4 was investigated as a reference sample (see Fig. 6). In Co_3O_4 the cobalt cation is present in the Co^{2+} state, tetrahedrally coordinated to the O^{2-}, and in the Co^{3+} state which is coordinated octahedrally to the oxygen anions with a Co^{3+}/Co^{2+} ratio of 2:1 [21]. In $CoAl_2O_4$, on the other hand, the oxidation state of the cobalt cation is 2. Due to these differences in the oxidation state, the Co $2p_{3/2}$ peak in the Co-XPS spectra of these two compounds differ strongly. In contrast to Co_3O_4, the Co $2p_{3/2}$ signal of $CoAl_2O_4$ exhibits a strong satellite structure on the higher binding energy side. This satellite structure can be ascribed to the shake-up process of the Co^{2+} compound in the high-spin state. In contrast, only a comparatively weak satellite

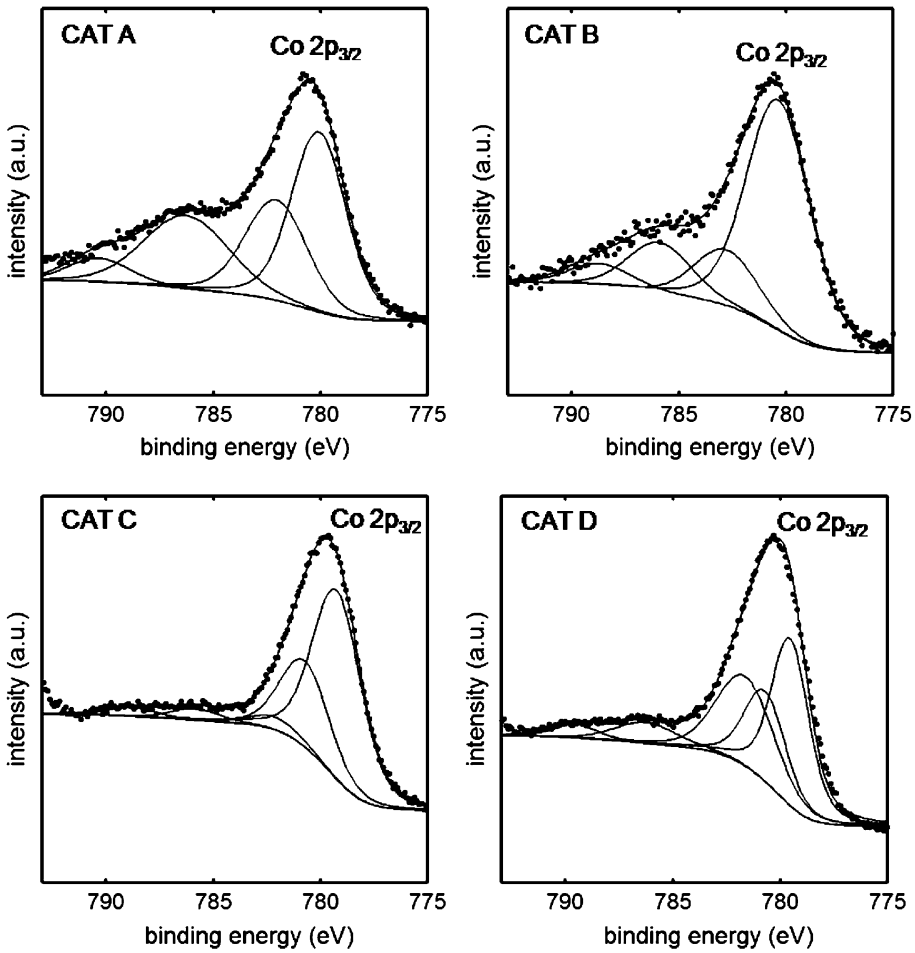

Fig. 5 High resolution XPS Co 2p spectra with curve fitting according to Table 4

Table 4 Fitted XPS binding energies of $Co(OH)_2$ and Co_3O_4 [23]

Co $2p_{3/2}$ (eV)	
$Co(OH)_2$	Co_3O_4
780.7	779.9
	781.2
782.5	782.5
786.3	785.5
790.7	789.8

structure associated with the Co $2p_{3/2}$ line can be observed for Co_3O_4 since the low-spin Co^{3+} ion does not show such a shake-up process [30] (see Fig. 5).

Comparing the four different samples with the pure Co_3O_4 reference sample (see Fig. 6), it turns out that CAT A and B differ strongly. Yang and co-workers [23] synthesised Co_3O_4 and $Co(OH)_2$, the latter as a sample compound in which the cobalt cation is present in the pure Co^{2+} state. Studying the two compounds with XPS they fitted the two Co 2p areas with a series of peaks varying in position and number. By investigating the Co 2p region in catalysts CAT A–D and applying the curve fitting parameters proposed in literature [23], we were able to show differences in the oxidation states of the cobalt cations in the four samples. Although all samples showed a predominant Co_3O_4 phase in the studies with Raman spectroscopy as well as XRD, in a the presence of a possibly amorphous $CoAl_2O_4$ phase, only the Co 2p area of CAT C and D could be fitted with the proposed fitting parameters for Co_3O_4. For samples CAT A and B the best fit was achieved by applying the peak positions proposed for $Co(OH)_2$ as a reference for a considerable amount of Co cations in the 2+ state. The Co^{2+} cations are known to incorporate into the alumina crystal lattice and form cobalt aluminates like $CoAl_2O_4$ [16, 31, 32]. The XPS results are therefore in close agreement with the TPR characterisations of the samples which also suggest that CAT A and B form hard to reduce cobalt species, or cobalt aluminate respectively.

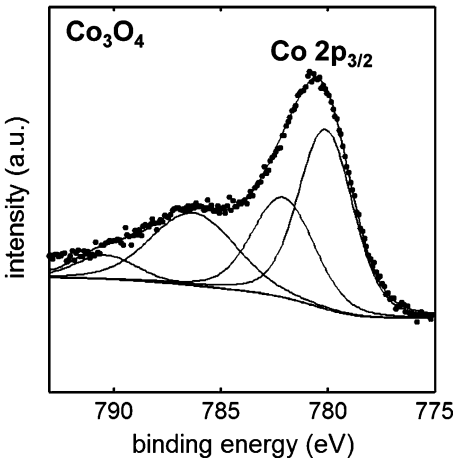

Fig. 6 High resolution XPS Co 2p spectra of Co_3O_4 reference material with curve fitting according to Table 4

4 Conclusions

In this study we could show, that the point of addition of the support during preparation plays a crucial role in the final composition of the supported cobalt oxide catalyst, while the temperature of the calcination/thermal treatment step does not seem to play the domination role (see methods C and D where different calcination temperatures were applied). The results suggest, that as soon as the alumina support comes into contact with the reverse micelle solution (Cat A and B), the probability of Co^{2+} ions being incorporated in the Al_2O_3 crystal lattice increases drastically. It has been reported that Al_2O_3 does dissolve in aqueous solutions at high pH [33, 34]. Although the pH in the whole solution is not expected to be this high, it is possible, that inside the confined geometry of the reverse micelles, the pH exceeds the dissolution limit temporarily. The mixture of dissolved Al^{3+} and unprecipitated Co^{2+} ions will form $CoAl_2O_4$ and other cobalt aluminates. Unprecipitated Co^{2+} could also be adsorbed on the alumina surface and be incorporated into its lattice upon thermal treatment. If the alumina is only contacted with the precipitate after extensive washing (CAT C and D), no cobalt aluminates could be observed. The difference in reduction behaviour between Cat C and D can be explained with the nature of the cobalt phase during the addition of the support. In method C the precipitated $Co(OH)_2$ could still be covered by residual surfactant resulting in an individual particle size being larger than the average pore diameter of the alumina ($đ_{pore} = 11.5$ nm). This only allows the particles to sit on the outer surface of the Al_2O_3 particle and having minimal interaction with the support. The Co_3O_4 crystallites prepared in Method D however are below 11.5 nm in diameter and can therefore penetrate the pores of the carrier. Inside the pores the cobalt oxide undergoes more interaction with the Al_2O_3 leading to a slightly higher reduction temperature. The results obtained give important information on how metal support interaction can be affected during preparation of reverse micelle derived supported catalysts.

References

1. Uskokovic V, Drofenik M (2007) Ad Coll Inter Sci 133:23–34
2. Uskokovic V, Drofenik M (2005) Surf Rev Lett 12:239–277.I
3. Eriksson S, Nylen U, Rojas S, Boutonnet M (2004) App Catal A Gen 265:207–219,and citations therein
4. Boutonnet M, Lögdberg S, Elm Svensson E (2008) Opin Coll Int Sci 13:270–286,and citations therein
5. Boutonnet M, Kizling J, Stenius P, Maire G (1982) Coll Surf 5:209–225
6. Jain R, Shukla D, Mehra A (2005) Langmuir 21:11528–11533
7. Natarajan U, Handique K, Mehra A, Bellare JR, Khilar KC (1996) Langmuir 12:2670–2678
8. Martinez A, Prieto G (2007) J Catal 245:470–476
9. Martinez A, Prieto G (2007) Catal Commun 8:1479–1486
10. Barkhuizen D, Mabaso I, Viljoen E, Welker C, Claeys M, van Steen E, Fletcher JCQ (2006) Pure App Chem 78:1759–1769
11. Mabaso EI, van Steen E, Claeys M (2006) DGMK/SCI-Conference "Synthesis Gas Chemistry" vol 4, pp 93–100
12. Mabaso EI (2005) Nanosized iron crystallites for Fischer–Tropsch synthesis, PhD, Department of chemical engineering, University of Cape Town, Cape Town
13. Cheang V (2009) Effect of crystallite size and water partial pressure on the activity and selectivity of low temperature iron-based Fischer-Tropsch catalysts, Department of Chemical Engineering, PhD, University of Cape Town, Cape Town
14. Lisiecki I (2005) J Phys Chem 109:12231–12244
15. Corolleur C, Tomanova D, Gault FG (1972) J Catal 24:401–416
16. Tavasoli A, Malek Abbaslou RM, Dalai AK (2008) Appl Catal A Gen 346:58–64
17. Fischer N, van Steen E, Claeys M (2011) Catal Tod 171:174–179
18. Welker CA (2007) Ruthenium based Fischer–Tropsch synthesis on crystallites and clusters of different sizes, Department of Chemical Engineering, PhD, University of Cape Town, Cape Town
19. Scarlett NVY, Madsen IC (2006) Powder Diffr 21:278–284
20. Kock LD, Waal DD (2007) J Raman Spectroc 38:1480–1487
21. Tang C-W, Wang C-B, Chien S-H (2008) Thermochim Acta 473:68–73
22. Hadjiev VG, Iliev MN, Vergilov IV (1988) J Phys C Solid State Phys 21:L199–L201
23. Yang J, Liu H, Martens WN, Frost RL (2009) J Phys Chem C 114:111–119
24. Jongsomjit B, Panpranot J, Goodwin JG (2001) J Catal 204:98–109
25. van Steen E, Sewell GS, Makhothe RA, Micklethwaite C, Manstein H, de Lange M, O'Connor CT (1996) J Catal 162:220–229
26. Arnoldy P, Moulijn JA (1985) J Catal 93:38–54
27. Todorova S, Zhelyazkov V, Kadinov G (1996) Reac Kin Catal Lett 57:105–110
28. Sewell GS, van Steen E, O'Connor CT (1996) Catal Lett 37:255–260
29. Sirijaruphan A, Horvath A, Goodwin JG Jr, Oukaci R (2003) Catal Lett 91:89–94
30. Xiong H, Zhang Y, Liew K, Li J (2005) J Mol Catal A Chemical 231:145–151

31. Saib AM, Borgna A, van de Loosdrecht J, van Berge PJ, Niemantsverdriet JW (2006) Appl Catal A Gen 312:12–19
32. Saib AM, Moodley DJ, Ciobîca IM, Hauman MM, Sigwebela BH, Weststrate CJ, Niemantsverdriet JW, van de Loosdrecht J (2010) Catal Tod 154:271–282
33. Al-Sheeha H, Marafi M, Stanislaus A (2008) Int J Min Proc 88:59–64
34. Grénman H, Salmi T, Murzin DY, Addai-Mensah J (2010) Hydrometallurgy 102:22–30